A Fast Discharge Scheme of Toroidal Field Coils for Fusion Demo Reactors

Yasuyuki ITOH[1)], Hiroyasu UTOH[2,3)], Yoshiteru SAKAMOTO[2,3)], Ryoji HIWATARI[2,3)] and Joint Special Design Team for Fusion DEMO[3)]

[1)]*Fukui University of Technology, Fukui 910-8505, Japan*

[2)]*National Institutes for Quantum and Radiological Science and Technology, Rokkasho, Aomori 039-3212, Japan*

[3)]*Joint Special Design Team for Fusion DEMO, Rokkasho, Aomori 039-3212, Japan*

(Received 5 August 2019 / Accepted 12 November 2019)

This paper describes an emergency fast discharge scheme of toroidal field (TF) coils of fusion demo reactors for reduction of induced voltage applied to turn insulations of conductors. TF coils are divided into serially connected segments that are electrically isolated from each other and only the coil segment having a failed coil is rapidly discharged. It was found from a circuit current analysis that this discharge scheme enables to reduce the insulation voltage with a factor of ~0.6 or less and which would contribute to ensure reliability of the turn insulations.

Keywords: nuclear fusion, toroidal field coil, quench, first discharge, turn insulation voltage, fusion demo reactor

DOI: 10.1585/pfr.14.1405167

1. Introduction

In emergency conditions of toroidal field (TF) coils of nuclear fusion devices, such as quench of superconductors, they must immediately discharge their current to suppress conductor temperature rising due Joule heating of copper stabilizers contained in strands.

In the case of ITER, the TF coil circuit consists of 9 cells connected in series with one power supply, where each cell has a pair of TF coils and a fast discharge unit (FDU) for the emergency shutdown [1]. The fast discharge of coils, however, generates a high induced voltage, which is applied to turn insulations. This voltage is proportional to the TF coil self-inductance for a given discharge time constant.

The ITER TF-coil set is operated with the conductor current of 68 kA and has the self-inductance of 17.3 H, the number of turns of $134 \times 18 = 2{,}412$, and the total initial FDU resistance of $9{\times}97\ \mathrm{m\Omega}{\sim}0.9\ \Omega$ [1,2]. These numerical values give the initial discharge time constant of 19 s. The turn-to-turn voltage is then calculated to be 26 V that gives the maximum insulation voltage between the radial plate and the conductor of 286 V [3].

The TF coil size of a fusion demo reactor called "JA DEMO", conceptually designed by the Joint Special Design Team for Fusion DEMO [4, 5], is about 1.4 times greater than ITER, which gives a 3 times greater self-inductance if the conductor current and the magnetic field strength are the same magnitudes as those of ITER and then generates a 3 times turn-insulation voltage that is quite capable of losing reliability of TF coils.

Because the self-inductance is proportional to a square of the number of turns, the increase in the conductor current is one of means for reducing the turn insulation voltage and is tried in the recent TF coil design of JA DEMO, where the conductor current is raised from 68 kA specified in the ITER TF coil design to 83 kA. The increasing in the discharge time constant also reduces the insulation voltage, which is however restricted because it causes the conductor temperature rise beyond its acceptable level in the coil quench event [6].

In this paper, we will present a fast discharge scheme of the TF coil current to reduce the insulation voltage without the increase in its time constant, dividing a set of TF coils into multi segments that are electrically isolated from each other.

2. Fast Discharge Scheme

2.1 Induced insulation voltage

The turn to turn voltage v_{TT} generated in the fast discharge of the TF coils is defined by

$$v_{TT} = L_0 I_{OP}/(N_T \tau_d) = I_{OP} R_0/N_T, \tag{1}$$

where L_0 is the TF coil self-inductance, I_{OP} the operating coil current, N_T the total number of turns, and τ_d the discharge time constant ($= L_0/R_0$ with R_0 being the total discharge resistance). The total number of turns is given by $N_T = n_C N_C$, where N_C is the number of TF coils and n_C the number of turns per coil. The conductor is wound in a double pancake along grooves of a radial plate (RP) with $2m$ turns. As in the ITER design [3], the RP is connected (through a resistor) to the conductor cross-over at

author's e-mail: y-itoh@fukui-ut.ac.jp

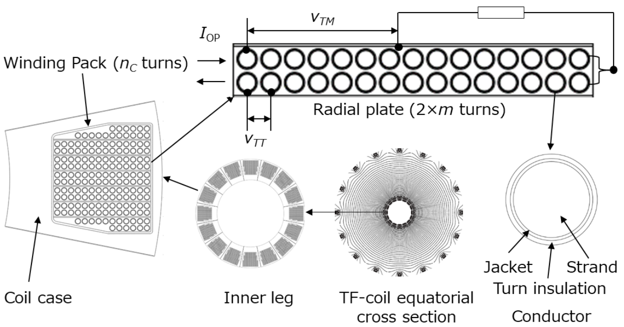

Fig. 1 Definitions of turn to turn voltage v_{TT} and maximum insulation voltage $v_{TM} = 2mv_{TT}$.

Table 1 Design parameters of TF coils for ITER and JA DEMO.

Item	ITER [1,2]	JA DEMO
Plasma major radius (m)	6.2	8.5
TF coil width (m)	9	12
TF coil height (m)	14	19
Self-inductance (H)	17.3	44.0
Maximum field strength (T)	11.8	13.8
Number of TF coils	18	16
Number of turns / coil	134	192
Operating current (kA)	68	83.2
Turn to turn voltage (V)	26	63.5
Maximum turn voltage (V)	286	953
Discharge time constant (s)	(19)(*)	←
Discharge resistance (Ω)	(0.92)(*)	2.35

(*) Estimated values

the plate edge (see Fig. 1) so that their potentials are equalized. Then the maximum turn insulation voltage v_{TM} is given by mv_{TT}, which is applied between the RP and the conductor jacket.

Table 1 presents design parameters of TF coils, which shows that the insulation voltage of JA DEMO is about three times greater than that of ITER for the same discharge time constant τ_d.

To reduce the maximum insulation voltage v_{TM}, we suppose to divide TF coils into M_C segments, where coils of the number $i = M_C(j-1)+k$, $(j = 1, \cdots, N_C/M_C$, $k = 1, \cdots, M_C)$, which belongs to the k-th segment, are serially connected and electrically isolated from coils with the different k (see Fig. 2). In this case, each coil segment is individually required to have a power supply.

Then, only the coil set having a failed coil, which is termed in the following as "*failed set*", is to be rapidly discharged. We also define the term "*intact set*" as the coil set in normal operating condition.

For example, when $M_C = 2$, one is a set of odd number coils and the other of even ones. In this case, the number of turns N_T is a half of the non-segmented coil set and the self-inductance L of the divided set of TF coils becomes a quarter of the non-segmented set because L is roughly proportional to the square of the number of turns,

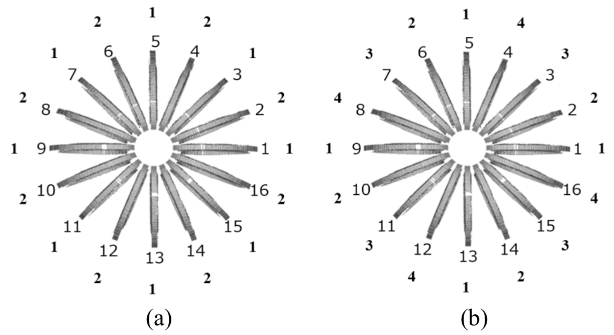

Fig. 2 Multi-segmentation of 16 TF coils, which are divided into (a) 2 segments (Two-divided TF coil sets) and (b) 4 segments (Four-divided TF coil sets), where numbers i of inside are of coils and those k of outside of coil segments.

Table 2 Values of self and mutual inductances $\bar{M}_{i,j}$ between i-th and j-th TF coils of JA Demo (i, j = 1 - 16, see Fig. 2).

$\|i-j\|$	0	1 or 15	2 or 14	3 or 13	4 or 12	5 or 11	6 or 10	7 or 9	8
$\bar{M}_{i,j}$(H)	1.0369	0.3832	0.1877	0.1052	0.0648	0.0436	0.0323	0.0267	0.0250

i.e., $L \sim L_0/M_C^2$. We therefore expect the turn to turn voltage v_{TT} to be halved according to Eq. (1).

The current of intact set, however, is magnetically coupled with that of the failed set, i.e., the intact set absorbs the magnetic flux of failed set losing its current, and increases beyond its acceptable level. Therefore, it is necessary to control the intact set current appropriately in this coil discharge scheme. To do this, we analyze time evolutions of the intact and failed set currents.

2.2 Two-divided TF coil sets

Coil currents I_i, $(i = 1, \cdots, M_C)$ are calculated for $M_C = 2$ by using circuit equations

$$\dot{I}_1 + \xi_1 \dot{I}_2 + \lambda_1 I_1 = 0 \text{ and } \dot{I}_2 + \xi_2 \dot{I}_1 + \lambda_2 I_2 = 0, \quad (2)$$

with $\xi_1 = M_{12}/L_1$, $\xi_2 = M_{21}/L_2$, $\lambda_1 = R_1/L_1$, and $\lambda_2 = R_2/L_2$, where R is the resistance, L the self-inductance, M the mutual inductance, and the subscript 1 denotes quantities of the failed coil set and 2 of the intact one.

Appendix A presents equations for calculating self and mutual inductances of divided coil segments with those of the non-segmented set of TF coils. For $M_C = 2$, we have $L_1 = L_2 = 13.05$ H and $M_{1,2} = M_{2,1} = 8.94$ H using mutual inductance values for JA DEMO presented in Table 2.

Figure 3 shows typical time evolutions of coil currents I_1 and I_2 to explain the scheme of fast discharge for the two-divided TF coil set, where the current I_0 of the non-segmented coil set is also shown for comparison, which is decayed with a time constant of τ_d, and all currents are equal to the operating current I_{OP} at the beginning of the

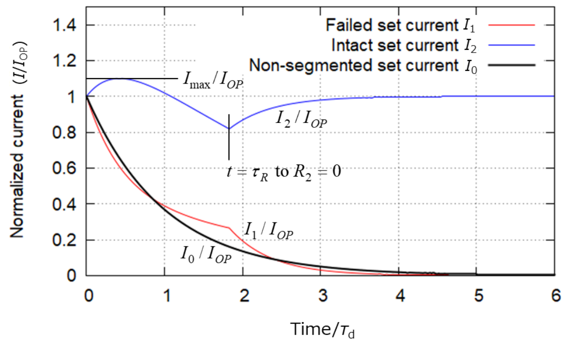

Fig. 3 Typical time evolutions of currents in fast discharge scheme of two-divided TF coil set, where the intact set is re-short-circuited ($R_2 = 0$) at $t = \tau_R$ so that it can rapidly absorb the magnetic flux released from the failed set.

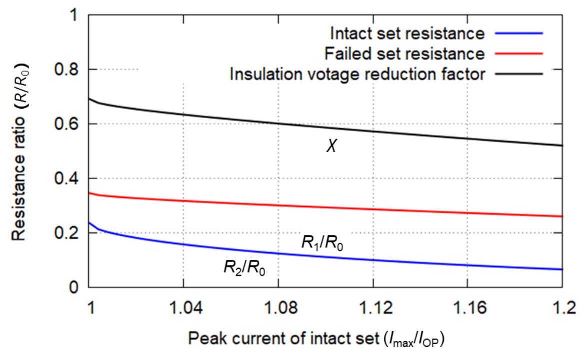

Fig. 4 Resistance ratios R_1/R_0 and R_2/R_0, and insulation voltage reduction factor χ for $M_C = 2$.

fast discharge.

When we choose resistance values under the condition of R_1 being sufficiently larger than R_2, the failed set current I_1 is more rapidly and monotonically decayed, whereas the intact set current I_2 initially increases with absorbing the magnetic flux released from the failed set and then start to decay after taking its maximum value $I_{\max}$ ($> I_{OP}$). Furthermore, I_2 increases again at $t = \tau_R$, when the resistance R_2 is removed from the intact set circuit, i.e., re-short-circuited, and asymptotically reaches a certain value that depends on τ_R.

Circuit parameters R_1, R_2, and τ_R for this discharge scheme are determined by the following conditions for given τ_d and $I_{\max}/I_{OP}$ with time functions of currents, $I_1(t)$ and $I_2(t)$ (see Appendix B):

$$\left.\begin{array}{l}\text{(a) } \int_0^\infty I_1^2(t)/I_{OP}^2 dt = \int_0^\infty I_0^2(t)/I_{OP}^2 dt = \tau_d/2 \\ \text{(b) } I_2(t)|_{t\to\infty}/I_{OP} = 1 \\ \text{(c) } \max(I_2(t)) = I_{\max}\end{array}\right\}. \quad (3)$$

The first condition (a) makes the effective decay time constant of the failed set current be that of the non-segmented TF coil set, τ_d, to roughly equalize their thermal impacts. The second one (b) is for the intact set to absorb the magnetic flux released from the failed set within their acceptable upper current limit to decay the current I_1 as fast as possible. For the third condition (c), the allowable value $I_{\max}$ of the current I_2 should be determined from viewpoints of stresses generated in coil structures and stability of superconductors.

Resistance ratios R_1/R_0 and R_2/R_0 calculated under conditions of Eq. (3) are presented in Fig. 4 as functions of $I_{\max}/I_{OP}$, where R_0 ($= L_0/\tau_d$) is the resistance of the non-segmented TF coil set. Figure 4 also shows the insulation voltage reduction factor χ, where χ is given by the ratio of the turn-to-turn voltage v_{TT} to that of the non-segmented TF coil set (v_{TT0}), i.e.,

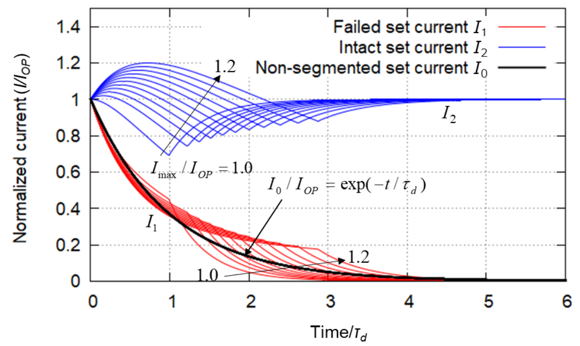

Fig. 5 Time evolutions of coil currents normalized by I_{OP} for $M_C = 2$ with I_{max}/I_{OP} as a parameter, where calculation parameters R_1, R_2, and τ_R were determined by Eq. (3) (see Figs. 3 and 4).

$$\chi = v_{TT}/v_{TT0} = \left(I_{op}R_1/(N_T/M_C)\right)/(I_{op}R_0/N_T)$$
$$= M_C R_1/R_0 \quad \text{with} \quad M_C = 2.$$

Resulting time evolutions of normalized coil currents I_1/I_{OP} and I_2/I_{OP} are shown in Fig. 5 with $I_{\max}/I_{OP}$ as a parameter. In this figure, the current increment $\Delta I_2 = I_{\max} - I_{OP}$ is proportional to the flux consumed and $\Delta I_2' = I_{OP} - I_2(\tau_R)$ to that stored by the intact set. We roughly see $(\Delta I_2 + \Delta I_2')/I_{OP}$~const. (~0.3) in Fig. 5, which is proportional to the total flux released by the failed set and absorbed by the intact set. The large ΔI_2 or $I_{\max}/I_{OP}$ can thus reduce the required resistance $R_1(\propto \chi)$ of the failed set for consuming its own flux, especially in the early stage of the discharge. The reduction factor χ is then decreased from 0.69 to 0.52 in the range of $1 \le I_{\max}/I_{OP} \le 1.2$ as shown in Fig. 4.

It would be necessary to estimate impacts of the transient overcurrent of the intact set on the TF coil structural integrity because it increases magnetic forces. The magnetic field generated by TF coils gives them the hoop force, which is expressed by the radial force F_R and the vertical force F_Z. Figure 6 shows their time evolutions for $I_{\max}/I_{op} = 1.1$ and 1.2. Because the failed set current I_1 is

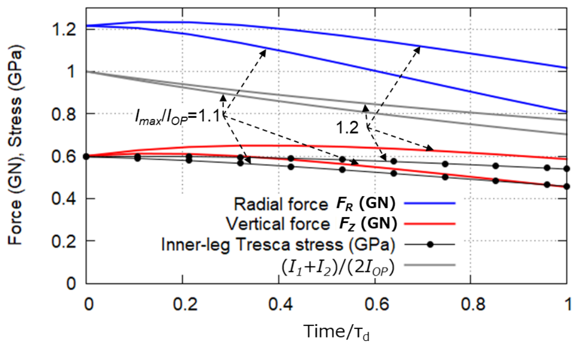

Fig. 6 Time evolutions of magnetic forces acting on TF coils and Tresca stress generated in inner-leg structures for $M_c = 2$.

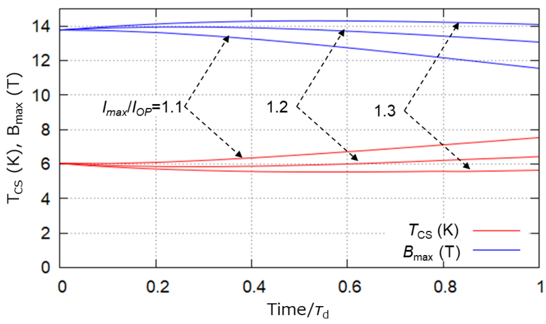

Fig. 7 Time evolutions of maximum field strength B_{max} on conductor axis and corresponding minimum current sharing temperature T_{CS} for $M_C = 2$.

rapidly decreasing, the increase in the local toroidal magnetic field during the overcurrent transient is not so much as I_2. Although appreciable increase is seen in the vertical force F_Z for $I_{\max}/I_{op} = 1.2$, it causes little increase in resulting stresses acting on inner-leg structures, as shown in Fig. 6.

We also estimated the decrease in the current sharing temperature T_{CS} [6] during the overcurrent transient of I_2. The current sharing temperature gives an index of upper temperature limit to keep the stability of super-conductors, at which the superconductor is in transition from superconducting state to normal one and the conductor current is shared by both the superconducting and normal-conducting (copper) strands.

Figure 7 shows time evolutions of maximum magnetic field strength $B_{\max}$ on the conductor axis and the corresponding minimum current sharing temperature T_{CS}, the latter of which is designed to be ~6 K for the TF coil conductor of JA DEMO. We see from Fig. 7 that the increase in $B_{\max}$ is small and therefore T_{CS} is hardly decreased for $I_{\max}/I_{op} \leq 1.2$.

Furthermore, we should pay attention to overturning forces acting on TF coils. These forces are generated by poloidal magnetic field that interacts with TF coil currents

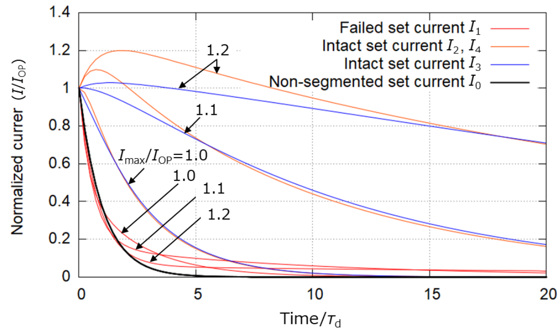

Fig. 8 Time evolutions of coil currents normalized by I_{OP} for $M_C = 4$ with $I_{\max}/I_{OP}$ as a parameter, where I_1 is of failed set to be rapidly discharged.

to cause toroidal forces in opposite directions across the TF coil equatorial plane. Since overturning forces are directly proportional to TF coil currents and $(I_1(t) + I_2(t))/(2I_{OP}) \leq 1$ at least for $I_{\max}/I_{op} \leq 1.2$, (see Fig. 6), net torques acting on inter-coil structures between coils of intact and failed sets are always small in comparison to those in the normal operation.

From these consideration using JA DEMO TF coil parameters, affects of the transient overcurrent of I_2 would be acceptable at least for $I_{\max}/I_{op} \leq 1.2$, which corresponds to the safe reduction factor $\chi \geq 0.52$. If we choose $I_{\max}/I_{op} > 1.2$, the peak magnetic field appreciably becomes greater than that in the normal operating condition as predicted from $B_{\max}$ curves drawn in Fig. 7, (e.g. $B_{\max} \to 14.3$ T for $I_{\max}/I_{op} = 1.3$), and the increase in the stress and the decrease in T_{CS} would not be ignored in considerations of the TF coil integrity and stability.

2.3 Four-divided TF coil sets

It is expected that the increase in the number M_C of coil segments reduces the insulation voltage more effectively because the rough estimation similar to Eq. (1) gives $v_{TT} \propto 1/M_C$. Figure 2 (b) shows coil segment numbers for $M_C = 4$. In this case, we need to calculate four coil currents I_k, ($k = 1$ - 4), where I_1 is the current of the failed coil set with the resistance of R_1 and currents I_k with $k = 2$ - 4 are for intact sets that are given the same discharge resistance R_2. Note that $I_2 = I_4$ because of geometrical symmetry in the positional relationship of coils with $k = 2$ and 4 (see Fig. 2 (b)).

We solved circuit equations for these currents numerically with $I_k(0) = I_{OP}$, ($k = 1$ - 4), and their results are shown in Fig. 8. In this case, intact sets were not re-short-circuited because the magnetic flux released from one failed coil set can easily be shared and consumed by residual three intact coil sets. Therefore intact set currents I_2, I_3, and I_4 in Fig. 8 are not re-increased, unlike Fig. 5 for $M_C = 2$.

Figure 9 shows required resistances R_1 and R_2 that satisfy conditions (a) and (c) of Eq. (3) with $\tau_R \to \infty$ and the

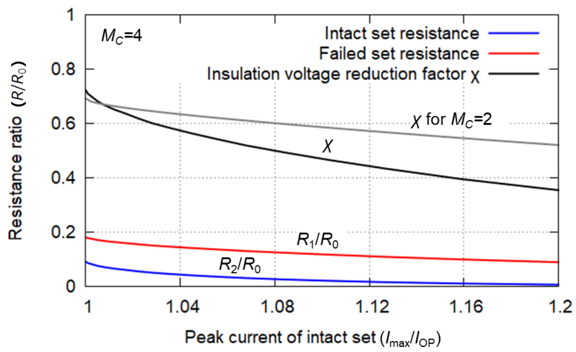

Fig. 9 Resistance ratios R_1/R_0 and R_2/R_0, and the reduction factor χ for $M_C = 4$ (without re-short-circuit) as functions of I_{max}/I_{OP}. The lower value of χ is obtained for $I_{max}/I_{OP} > 1.01$ in comparison to $M_C = 2$.

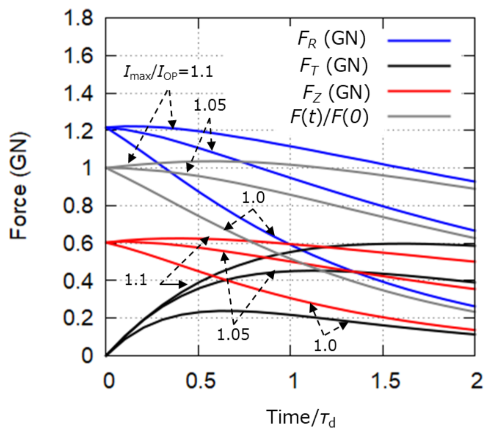

Fig. 10 Time evolutions of magnetic forces F_R, F_T, and F_Z acting on TF coils with segment number of 2 or 4, where $F(t) = (F_R^2(t) + F_T^2(t) + F_Z^2(t))^{1/2}$.

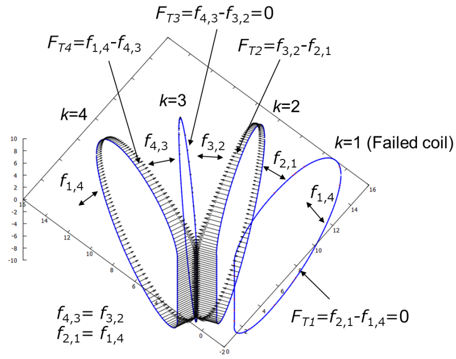

Fig. 11 Distribution of toroidal component of magnetic force (arb. unit) per unit length generated by fast discharge with $M_C = 4$ and $I_{max}/I_{OP} = 1$, where $f_{i,j}$, (i, j = 1 - 4) is the magnetic attractive force between i-th and j-th coil currents and $F_{Tk} = f_{k+1,k} - f_{k,k-1}$ is the net toroidal force acting on k-th coil.

insulation voltage reduction factor $\chi = 4R_1/R_0$, where we see that χ is always lower than that of $M_C = 2$ except for $I_{\max}/I_{OP} < 1.01$. This result makes us have a high expectation for $M_C = 4$ to obtain a smaller value of χ even without the re-short-circuiting.

Figure 10 shows magnetic forces acting on TF coils that belong to the coil segment with the number k of 2 or 4, of which current takes a peak value as shown in Fig. 7. There is no problem in the hoop force (radial and vertical forces) for $I_{\max}/I_{OP} \leq 1.1$. However, the toroidal force is generated in intact coil segments with the number k of 2 and 4. This reason is that only the current of failed coil segment with $k = 1$ is decreased more rapidly than those of intact ones as seen from Fig. 8. Figure 11 shows the distribution of the toroidal force per unit length of TF coils with $k = 2$ and 4.

In Fig. 11, the attractive force $f_{3,2}$ generated between coil currents I_2 and I_3 or $f_{4,3}$, between I_3 and I_4 is greater than $f_{2,1}$ between I_1 and I_2 or $f_{1,4}$ between I_4 and I_1. Resultantly, the net toroidal forces F_{T2} and F_{T4} are generated on coils of $k = 2$ and 4, respectively, unlike the case of $M_C = 2$ that generates the same attractive force between adjacent coils. On the other hand, no toroidal force is generated on coils of $k = 1$ and 3 because of the geometrical symmetry that gives $f_{4,3} = f_{3,2}$ and $f_{2,1} = f_{1,4}$.

We see from Fig. 10 that the toroidal force F_T becomes the same order of magnitude as the hoop force (F_R, F_Z) acting on TF coils at $t \sim \tau_d$. This force would generate additional stresses in the coil case and the RP except for $k = 1$, especially near the inner leg (see Fig. 11).

For example, the toroidal force F_T becomes ~400 MN at $t \sim 0.5\tau_d$ for $I_{\max}/I_{OP} = 1.1$ with the radial and vertical forces (F_R and F_Z) being still nearly the same values as those of the normal operation. Then, we roughly estimate the additional toroidal stress generated in the RP to be several tens MPa, using the current center line length of the TF coil~50 m, the coil width~1.6 m, and the RP metal occupation factor ~0.15. This additional stress would be intolerable for the coil design.

Here we define a force vector (F_R, F_T, F_R) acting on the coil mass center. If $dF(t)/dt \leq 0$ with $F(t) = (F_R^2(t) + F_T^2(t) + F_Z^2(t))^{1/2}$ (see Fig. 10) can be used as a condition for keeping the stress within its designed value, we roughly estimate the acceptable range as $1 \leq I_{\max}/I_{OP} \leq 1.05$ that gives the minimum reduction factor $\chi \sim 0.55$.

It should be noted that this toroidal force generation makes the re-short-circuiting be unacceptable for $M_C = 4$, because final values of currents become $I_1 = 0$ and $I_k = I_{OP}$, (k = 2 - 4), which gave $F(t \to \infty) = 1.13F(0)$.

2.4 Discussions

Two fast discharge schemes of multi-segmented TF coils have been considered with $M_C = 2$ and 4.

The discharge scheme with $M_C = 4$ decays the failed set current more efficiently in comparison to that with

$M_C = 2$ even without the re-short-circuiting that requests additional high direct-current switching components and their control units.

However, there is a sever problem for the $M_C = 4$ segmentation to generate the toroidal force. It causes additional stresses in coil structures and restricts the increase in $I_{\max}/I_{OP}$ for achieving the high reduction factor to ~1.05 that gives $\chi = 0.55$, whereas the case of $M_C = 2$ allows it to be ~1.2 with $\chi = 0.52$. This force would also request reinforcement of inter-coil supporting structures of TF coils.

Comprehensively the discharge scheme would prefer to select $M_C = 2$ rather than $M_C = 4$ for achieving a lower reduction factor of the insulation voltage.

3. Summary

An emergency fast discharge scheme of TF coils for fusion demo reactors has been considered to reduce induced voltage applied to turn insulations. In this scheme, TF coils are divided into multiple segments that are individually connected serially and electrically isolated from each other.

Each coil segment has a pair of discharge resistors R_1 and R_2 with $R_1 > R_2$. In an emergency condition, the coil segment having a failed coil is serially connected to R_1 and other segments (intact sets) to R_2 and thus only the coil segment that includes a failed coil is discharged more rapidly.

The intact set then has a role of absorbing the magnetic flux released from the failed set and therefore its currents is initially increased. To enhance this action and decay the failed set current more rapidly, the resistor R_2 connected to the intact set is removes again (re-short circuiting) at an appropriate timing in the case of the two-divided coil set ($M_C = 2$).

It was found from the circuit current analysis for JA DEMO TF coil parameters that the insulation voltage can be reduced by the factor χ of 0.6 or less (minimum 0.52 for $M_C = 2$) within the transient overcurrent of the intact set being tolerable level.

The four-divided set ($M_C = 4$) seems to reduce the factor χ more effectively. However, this scheme has no advantage compared to the case for $M_C = 2$ because of the toroidal force generation that causes additional stresses in coil structures and thus prevents the decrease in χ.

Acknowledgments

This work was conducted in the framework of the Joint Special Design Team for Fusion DEMO collaboration program with National Institutes for Quantum and Radiological Science and Technology, Japan.

[1] ITER Design Description Document, DDD 11, Magnet, 8. Fault and Safety Analysis, Annex 6a, "Assessment of the TF coil Circuit Behavior during Normal and Fault Conditions", Bareyt, B; N 41 RI 34 00-11-01 W 0.1 (2009).
[2] ITER Design Description Document, DDD 11, Magnets, 2. TF coils and Structures, ITER_D_ 2MVZNX v2.2 (2009).
[3] ITER Design Description Document, DDD 11, Magnet, 1. Design Basis, ITER_D_2NPLKM v1.8 (2009).
[4] Japan Home Team *et al.*, "Second Intermediate Report of BA DEMO Design Activity" (2017).
[5] K. Tobita *et al.*, "Japan's Efforts to Develop the Concept of JA DEMO During the Past Decade", Fusion Sci. Technol. (2019) 1943-7641.
[6] ITER Design Description Document, DDD 11, Magnets, 7. Conductors, ITER_D_2NBKXY v1.2 (2009).

Appendix A. Inductances of Divided Coil Set

The self-inductance and the mutual inductance in Eq. (2) are calculated for $M_C = 2$ by $L_1 = L_2 = M^*_{1,1}$ $(= M^*_{2,2})$, $M_{1,2} = M_{2,1} = M^*_{1,2}$ $(= M^*_{2,1})$, where

$$M^*_{i,j}\ (= M^*_{j,i}) = (N_C/M_C) \sum_{k=1}^{N_C/M_C} \bar{M}_{i,M_C(k-1)+j},$$

with $\bar{M}_{i,j}$ $(= \bar{M}_{j,i})$, $(i, j = 1, \cdots, N_C)$, being mutual inductances of the non-segmented set of TF coils, values of which are presented in Table 2.

Appendix B. Solutions of Circuit Equations

Solutions of circuit equations Eq. (2) for $M_C = 2$ with initial conditions of $I_1(0) = I_2(0) = I_{\rm OP}$ are obtained for $t \le \tau_R$ to be

$$I_1/I_{OP} = \gamma_{12}e^{-\alpha_1 t} - \gamma_{22}e^{-\alpha_2 t} \text{ and}$$
$$I_2/I_{OP} = \gamma_{11}e^{-\alpha_1 t} - \gamma_{21}e^{-\alpha_2 t},$$
$$\text{where } \alpha_i = X\left(1 - (-1)^i(1 - Y)^{1/2}\right) \text{ and}$$
$$\gamma_{ij} = 2^{-1}\left((1 - Z_j)(1 - Y)^{-1/2} - (-1)^i\right) \text{ with}$$
$$X = \frac{\lambda_1 + \lambda_2}{2(1 - \xi^2)},\ Y = \frac{4\lambda_1\lambda_2(1 - \xi^2)}{(\lambda_1 + \lambda_2)^2},$$
$$\text{and } Z_j = \frac{2\lambda_j(1 + \xi)}{(\lambda_1 + \lambda_2)},$$
$$(i, j = 1, 2 \text{ and } \xi = \xi_1 = \xi_2).$$

For $t > \tau_R$, coil currents are calculated from circuit equations Eq. (2) with $\lambda_2 = R_2/L_2 = 0$ by

$$I_1(t) = I_1(\tau_R)\exp\left(-\lambda_1(t - \tau_R)/\left(1 - \xi^2\right)\right) \text{ and}$$
$$I_2(t) = I_2(\tau_R) + \xi\left(I_1(\tau_R) - I_1(t)\right).$$